Chapter 10
The Coupled Cluster Method

Abstract Another powerful method of quantum many theory that obeys the linked-cluster theorem, and so provides results for the infinite lattice from the outset, is the Coupled Cluster Method (CCM). It has previously been applied to a wide range of quantum systems. We show here how it can be applied to quantum spin systems. The CCM formalism is described in detail. Crucial to understanding the CCM is the role of the model state upon which clusters of spin-raising operators act in order to form the basis states. Various approximation schemes may be used in order to calculate expectation values in practical calculations, examples being the LSUBm and SUBm approximation schemes. The LSUB2 and SUB2 approximations are presented in detail. Results for the LSUB2 approximation for the spin-half Heisenberg model on the linear chain are shown to be improved when compared to those of classical theory. We demonstrate how the CCM may be applied in order to study the ground- and excited-state properties of the anisotropic (XXZ) Heisenberg model on the square lattice. The CCM is shown is to provide an accurate and coherent picture for this model.

10.1 Introduction

In this chapter we consider another method that gives accurate results in the infinite lattice limit, especially for spin systems of two spatial dimensions, known as the coupled cluster method (CCM) [1]. The CCM is a well-known and widely applied method of quantum many-body theory. It allows us to calculate expectation values for the infinite lattice, which is a clear advantage to the method.

However, an aspect of the method is that one must often make an approximation within the bra- and ket-state wave functions, even though we obtain results in the infinite-lattice limit from the outset. The manner in which we construct these approximations is discussed below. Only lower orders of approximation than series expansions are possible, although the CCM contains many more diagrams than series expansions at "corresponding" levels of approximation. Furthermore, one does not necessarily obtain an upper bound on the ground-state energy using the CCM and no rules exist for extrapolation. Despite this, however, it is remarkable

Parkinson, J.B., Farnell, D.J.J.: *The Coupled Cluster Method*. Lect. Notes Phys. **816**, 109–134 (2010)
DOI 10.1007/978-3-642-13290-2_10 © Springer-Verlag Berlin Heidelberg 2010

that the CCM still has been shown to provide consistently accurate results for a variety of quantum problems and for a wide range of expectation values (see final chapter). The CCM has been also applied with much success to quantum spin systems [2–10]. and it may be applied in the presence of even very strong frustration. Recent advances in the method have concentrated in applying it to high orders of approximation via computational methods [6–9].

10.2 The CCM Formalism

The first step in the coupled cluster method is to select an appropriate *model* state $|\Phi\rangle$. This state should be ideally be (i) simple and (ii) a reasonable starting approximation to the true ground state. The model state is assumed to act as a *vacuum* state so that a complete basis for any state can be constructed by operating on it by *creation* operators c_i^+. These creation operators act at a single lattice site i and a general state is obtained by operating on the model state with a linear combination of products of creation operators. We shall denote a product of creation operators, acting in general at several different sites, as C_I^+.

The central idea underpinning the CCM is to obtain better and better approximations to the true ground state $|\Psi\rangle$ by modifying the wave function in a systematic way, namely, by building in more and more of the true correlations with respect to the model state. Clearly there must be an operator P such that

$$|\Psi\rangle = P|\Phi\rangle. \tag{10.1}$$

However, rather than try to calculate P directly, we choose to introduce a new operator S where $P = e^S$ and attempt to calculate S instead. At first sight this seems an additional complication but the reason for it is as follows. By using this form it can be shown that any approximation we make by truncating S has the property that the equivalent diagrammatic perturbation theory approximation involves a summation only over *linked* diagrams. This is important since the Goldstone theorem states that only linked diagrams should be included if the calculated extensive property is to scale linearly with N, the size of the system.

It can be shown that the operator P and also the operator S consist of a sum of terms, where each term is itself a product of creation operators only, with respect to the model state. In the context of the Heisenberg model on a bipartite lattice such as the linear chain or square lattice, a creation operator is a spin-raising operator for sites where the spin is down or a spin lowering operator for sites where the spin is up. These creation operators are all mutually commuting. Hence, we write S as

$$S = \sum_{I \neq 0} S_I C_I^+, \tag{10.2}$$

where C_I^+ is a product of creation operators with associated (ket-state) correlation coefficient S_I.

For the exact ground state $|\Psi\rangle$

$$\mathcal{H}|\Psi\rangle = E_g|\Psi\rangle \quad \text{and} \quad \langle\tilde{\Psi}|\mathcal{H} = E_g\langle\tilde{\Psi}|, \tag{10.3}$$

where E_g is the exact ground state energy and $\langle\tilde{\Psi}|$ is the Hermitian conjugate of $|\Psi\rangle$. However, since we are writing

$$|\Psi\rangle \;=\; P|\Phi\rangle \;=\; e^S|\Phi\rangle, \tag{10.4}$$

and in most cases, S is an approximation to the true S, $|\Psi\rangle$ is an approximate ground state. It is obtained typically by truncating the otherwise infinite series of terms in S. Furthermore, we do not assume that the approximate $\langle\tilde{\Psi}|$ is the Hermitian conjugate of the approximate $|\Psi\rangle$. In fact, we shall construct $\langle\tilde{\Psi}|$ using a new auxiliary operator $\tilde{S}$ which is constructed from destruction operators only. $\tilde{S}$ is not the Hermitian conjugate of S and has to be obtained separately. The basic formulas are

$$|\Psi\rangle = \mathrm{e}^S|\Phi\rangle \quad S = \sum_{I\neq 0} \mathcal{S}_I C_I^+, \tag{10.5}$$

$$\langle\tilde{\Psi}| = \langle\Phi|\tilde{S}\mathrm{e}^{-S} \quad \tilde{S} = 1 + \sum_{I\neq 0} \tilde{\mathcal{S}}_I C_I^-. \tag{10.6}$$

This method of treating the bra state, using a linear operator $\tilde{S}$, is known as the normal coupled cluster method (NCCM). An alternative treatment is known as the Extended coupled cluster method (ECCM) in which the bra state is calculated using an exponentiated operator. The reader is referred to [11] for further details.

As mentioned earlier, the model or reference state $|\Phi\rangle$ plays the role of a vacuum state with respect to the $\{C_I^+\}$, i.e. their Hermitian conjugates $\{C_I^-\}$, have the property that $C_I^-|\Phi\rangle = 0, \forall\, I \neq 0$. We define that $C_0^+ \equiv C_0^- \equiv 1$ to be the identity operator. Furthermore, the set $\{C_I^+\}$ is complete and consists of all possible products of creation operators on multiple sites.

Also as mentioned earlier, the correlation operator S is composed entirely of the creation operators $\{C_I^+\}$, and these operators, acting on the model state, create other states in the relevant basis which are then mixed in to the model state to form an approximation to the 'true' ground state. Note that although the Hermiticity of the true ground state is lost, i.e. $\langle\tilde{\Psi}|^\dagger \;\neq\; |\Psi\rangle/\langle\Psi|\Psi\rangle$, we can still impose the normalisation conditions $\langle\tilde{\Psi}|\Psi\rangle \;=\; \langle\Phi|\Psi\rangle \;=\; \langle\Phi|\Phi\rangle \;\equiv\; 1$. The coefficients $\{\mathcal{S}_I\}$ and $\{\tilde{\mathcal{S}}_I\}$ are known as the ket- and bra-state *correlation coefficients*, respectively.

In general we need both $|\Psi\rangle$ and $\langle\tilde{\Psi}|$ (and hence need both $\{\mathcal{S}_I\}$ and $\{\tilde{\mathcal{S}}_I\}$) in order to find the ground-state expectation value of any operator, although the ground-state energy E_g is a special case which only requires knowledge of the $\{\mathcal{S}_I\}$.

For an arbitrary operator A the expectation value is given by,

$$\bar{A} \;\equiv\; \langle\tilde{\Psi}|A|\Psi\rangle \;=\; \langle\Phi|\tilde{S}\mathrm{e}^{-S}A\mathrm{e}^S|\Phi\rangle \;=\; \bar{A}\left(\{\mathcal{S}_I, \tilde{\mathcal{S}}_I\}\right). \tag{10.7}$$

The similarity transform of the operator A, occurring here and denoted by $\hat{A}$, may be written as a series of nested commutators:

$$\hat{A} \equiv e^{-S} A e^{S} = A + [A, S] + \frac{1}{2!}[[A, S], S] + \cdots \tag{10.8}$$

In this expression each commutation reduces the number of destruction operators by one. As these commutations are nested within each other, the series will terminate at finite order provided that the operator A contains only a finite number of destruction operators. (There is no limit on the number of creation operators in A). N.B. we use the notation $\hat{}$ for a similarity transformed operator; we use the notation $\bar{}$ for an expectation value and the symbol $\tilde{}$ for the bra-state, its correlation operator $\tilde{S}$ and the corresponding coefficients $\{\tilde{S}_I\}$.

Using (10.3) and (10.4)

$$\mathcal{H} e^{S} |\Phi\rangle = E_g e^{S} |\Phi\rangle \tag{10.9}$$

$$\therefore \quad e^{-S} \mathcal{H} e^{S} |\Phi\rangle = E_g |\Phi\rangle \tag{10.10}$$

$$\text{i.e.} \quad \hat{\mathcal{H}} |\Phi\rangle = E_g |\Phi\rangle \tag{10.11}$$

from which it immediately follows, using the normalisation $\langle \Phi | \Phi \rangle = 1$, that

$$E_g = \langle \Phi | \hat{\mathcal{H}} | \Phi \rangle \tag{10.12}$$

From (10.10) $C_I^- e^{-S} \mathcal{H} e^{S} |\Phi\rangle = E_g C_I^- |\Phi\rangle = 0$ since any destruction operator C_I^- acting on the vacuum state $|\Phi\rangle$ gives zero. Thus finally

$$\langle \Phi | C_I^- e^{-S} \mathcal{H} e^{S} | \Phi \rangle = \langle \Phi | C_I^- \hat{\mathcal{H}} | \Phi \rangle = 0. \tag{10.13}$$

By choosing different C_I in Eq. (10.13) one obtains a coupled set of non-linear multinomial equations for the correlation coefficients $\{\mathcal{S}_I\}$.

Also, using (10.3) and (10.6),

$$\begin{aligned}
\langle \Phi | \tilde{S} e^{-S} \mathcal{H} &= E_g \langle \Phi | \tilde{S} e^{-S} \\
\langle \Phi | \tilde{S} e^{-S} \mathcal{H} C_I^+ &= E_g \langle \Phi | \tilde{S} e^{-S} C_I^+ \\
\langle \Phi | \tilde{S} e^{-S} \mathcal{H} C_I^+ e^{S} | \Phi \rangle &= E_g \langle \Phi | \tilde{S} e^{-S} C_I^+ e^{S} | \Phi \rangle \\
&= \langle \Phi | \tilde{S} e^{-S} C_I^+ \mathcal{H} e^{S} | \Phi \rangle \quad \text{using (10.9)} \\
\therefore \quad \langle \Phi | \tilde{S} e^{-S} [\mathcal{H}, C_I^+] e^{S} | \Phi \rangle &= 0
\end{aligned} \tag{10.14}$$

By choosing different C_I^+ in this equation one obtains a coupled set of *linear* multinomial equations for the correlation coefficients $\{\mathcal{S}_I\}$.

For many purposes these three Eqs. (10.12), (10.13) and (10.14), together with (10.4), (10.5) and (10.6) form the essential core of the CCM method.

It is important to realise that, unlike conventional variational methods, this bi-variational formulation does *not* lead to an upper bound for E_g when the series in S and $\tilde{S}$ of Eqs. (10.5) and (10.6) are truncated. This is due to the lack of exact Hermiticity when such approximations are made.

The nested commutator expansion of the similarity-transformed Hamiltonian is given by

$$\hat{\mathcal{H}} \equiv e^{-S}\mathcal{H}e^{S} = \mathcal{H} + [\mathcal{H}, S] + \frac{1}{2!}[[\mathcal{H}, S], S] + \cdots . \tag{10.15}$$

This equation and the fact that all of the individual components of S in the sum in Eq. (10.5) commute with one another together imply that each element of S in Eq. (10.5) is linked directly to the Hamiltonian in each of the terms in Eq. (10.15). Equation (10.15) is therefore of *linked-cluster* type. As noted above, each of these equations is of finite length when expanded because the otherwise infinite series in Eq. (10.15) must always terminate at a finite order, provided only that each term in $\mathcal{H}$ contains a finite number of single-body destruction operators. Hence, the CCM parametrisation naturally leads to a workable scheme that can be carried out by hand for low orders of approximation or implemented computationally for higher orders of approximation. We stress that the similarity transformation lies at the heart of the CCM. This is in contrast to the *unitary* transformation that is at the heart of the standard variational formulation in which the bra state $\langle\tilde{\Psi}|$ is simply taken as the explicit Hermitian conjugate of $|\Psi\rangle$.

For the case of spin-lattice problems of the type considered here, the model state is usually the Néel state. Furthermore, it is useful to carry out a local rotation of the local spin axes at the 'up' sites so that these spins are all notionally pointing 'down'. This is purely a mathematical device; there is no physical rotation of the spins themselves but rather of the local axes we use to measure them. However, this does ensure that all the 'creation' operators with respect to the model state are now spin-raising operators of the form s_k^+ and the operators C_I^+ become products of these spin-raising operators only. This is very useful from a formal point of view because we treat all spins in exactly the same way regardless of whether they are on one sublattice or another.

We note that the CCM formalism would be exact if all possible multi-spin cluster correlations for S and $\tilde{S}$ were included. In any real application this is usually impossible to achieve. We remark again that it is therefore necessary to approximate the ground-state wave function. Indeed, we are able to construct approximation schemes within S and $\tilde{S}$ in which the number and/or type of clusters retained is restricted. The three most commonly employed schemes are:

(1) the **SUB***n* scheme, in which all correlations involving only n or fewer spins are retained, but no further restriction is made concerning their spatial separation on the lattice;
(2) the **SUB***n*-*m* sub-approximation, in which all SUBn correlations spanning a range of no more than m adjacent lattice sites are retained; and

(3) the localised **LSUB***m* scheme, in which all multi-spin correlations over all distinct locales on the lattice defined by m or fewer contiguous sites are retained. The problem of solving for these types of approximation schemes using analytical and computational approaches is discussed below.

All of these approximation schemes follow the 'rule' that defines a true quantum many-body theory, namely, that we may increase the level of approximation in a systemic and well-controlled manner. Furthermore, we can also attempt to extrapolation our 'raw' SUBn, SUBn-m, and LSUBm results in the limits $n, m \to \infty$. However, by contrast to exact diagonalisations and quantum Monte Carlo in which finite-sized lattice results are extrapolated in the infinite lattice limit using well-defined extrapolation procedures, no such equivalent extrapolation schemes exist as yet for the CCM. We are therefore forced to use 'heuristic' or 'ad hoc' schemes in order to extrapolate our results. An example of an 'heuristic' extrapolation scheme of LSUBm data for the ground state energy is a polynomial fit given by $y = a + bm^{-2} + cm^{-4}$. A similar polynomial fit for the sublattice magnetisation is $y = a + bm^{-1} + cm^{-2}$, although a power-law fit, i.e., $y = a + bm^{-v}$, is also often used in this case. The lack of an upper bound on the ground-state energy (due to the fact that bra and ket states are not explicitly constrained to be Hermitian conjugates) is not the biggest problem in practice. Indeed, the CCM often does provide an upper bound for those cases in which the model state is believed to be a reasonable "starting point." In fact, the biggest limitation of the CCM in practice is the lack of concrete "rules" for extrapolation of LSUBm results and the (sometimes) rather small number of LSUBm results to extrapolate with – even with intensive computer methods. However, it is remarkable that, despite these potential limitations, the CCM often does provide accurate results compared to results of exact studies and the best of other approximate methods. This is demonstrated later on in this chapter and also in the next.

The NCCM may also be used to investigate excited states. In order to do this we introduce a third *excited-state* operator X^e (in addition to the CCM ground-state ket- and bra-state operators, S and $\tilde{S}$). This operator is again a linear combination of the C_I^+ with associated coefficients $\{\mathcal{X}_I^e\}$

$$X^e = \sum_{I \neq 0} \mathcal{X}_I^e C_I^+. \tag{10.16}$$

We see readily that X^e commutes with S as it contains only the set $\{C_I^+\}$ of multi-spin creation operators. However, the specific clusters used in the set $\{C_I^+\}$ may differ from those used in the ground-state parametrisation in Eqs. (10.5) and (10.6) if the excited state has different quantum numbers than the ground state. An excited-state wave function, $|\Psi_e\rangle$, is determined by applying X^e to the ket-state wave function of Eq. (10.5) such that

$$|\Psi_e\rangle = X^e\, e^S |\Phi\rangle. \tag{10.17}$$

The energy E_e of the excited state is given by the Schrödinger equation, where

$$\mathcal{H}|\Psi_e\rangle = E_e|\Psi_e\rangle. \tag{10.18}$$

We may apply X^e to the CCM ground-state Schrödinger equation such that $X^e\mathcal{H}|\Psi\rangle = E_g X^e|\Psi\rangle$. This expression, in turn, leads to

$$\begin{aligned} E_e|\Psi_e\rangle - E_g X^e|\Psi\rangle &\equiv \mathcal{H}|\Psi_e\rangle - X^e\mathcal{H}|\Psi\rangle \\ \Rightarrow E_e X^e e^S|\Phi\rangle - E_g X^e e^S|\Phi\rangle &= \mathcal{H}X^e e^S|\Phi\rangle - X^e\mathcal{H}e^S|\Phi\rangle \\ \text{or } \varepsilon_e X^e|\Phi\rangle &= e^{-S}[\mathcal{H}, X^e]e^S|\Phi\rangle, \end{aligned} \tag{10.19}$$

where $\varepsilon_e \equiv E_e - E_g$ is the excitation energy and we note that $[X^e, e^S] = 0$. Equation (10.17) implies that $\langle\Phi|\Psi_e\rangle = 0$. Thus, we find by applying $\langle\Phi|C_I^-$ to Eq. (10.19) that,

$$\varepsilon_e \mathcal{X}_I^e = \langle\Phi|C_I^- e^{-S}[\mathcal{H}, X^e]e^S|\Phi\rangle, \forall\, I \neq 0, \tag{10.20}$$

which is a generalised set of eigenvalue equations with eigenvalues ε_e and corresponding eigenvectors $\mathcal{X}_I^e$, for the excited states.

Again, we note that it is sometimes possible to solve these sets of equations by hand for low orders of approximation. However, it rapidly becomes clear that analytical determination of the CCM equations for higher orders of approximation is impractical and it is therefore necessary to employ computer algebraic techniques both to determine and to solve the equations. Once the bra- and ket-state equations have been determined they are readily solved using standard techniques for the solution of coupled polynomial equations (e.g., the Newton-Raphson method). The excited-state eigenvalue equations may be also determined and solved computationally thereafter. A full description of the details in applying the CCM to high orders of approximation is given for the ground state in Bishop et al. [7]. We have seen above that we are able to increase the level of approximation for the the SUBn, SUBm-m and LSUBm approximation schemes in in the ground state in a systematic way. This holds true also for the excited states. Thus, excited-state energies may again be extrapolated to the 'exact limit' $n, m \to \infty$ using a variety of 'heuristic' approaches.

10.3 The XXZ-Model

In this chapter we shall use lower case s^z, etc., for spin operators to avoid confusion with the capital S and $\tilde{S}$ which are the CCM correlation operators.

The spin-half XXZ antiferromagnetic model on the square lattice has a Hamiltonian given by

$$\mathcal{H} = \sum_{\langle i,j\rangle}[s_i^x s_j^x + s_i^y s_j^y + \Delta s_i^z s_j^z] = \frac{1}{2}\sum_{\langle i,j\rangle}[s_i^+ s_j^- + s_i^- s_j^+ + 2\Delta s_i^z s_j^z], \tag{10.21}$$

where the sum on $\langle i, j\rangle$ counts all nearest-neighbour pairs once. The Néel state, with all 'down' spins on one sublattice and all 'up' spins on the other, is the ground state in the (trivial) Ising limit $\Delta \to \infty$. As Δ decreases the ground state remains Néel-like until a phase transition occurs at (or near to) $\Delta = 1$. By Néel-like we mean that there is a substantial positive expectation value of $\langle s^z\rangle$ for spins on one sublattice and an equal and opposite expectation value for those spins on the other. Even at $\Delta = 1$ (i.e., the Heisenberg model), approximately 61% to 62% of the classical ordering remains in the quantum system. For $-1 < \Delta < 1$ the ground state is co-planar, with zero expectation value for $\langle s^z\rangle$; the atoms are aligned in the xy-plane. For $\Delta < -1$ the system is ferromagnetic and the exact ground state has all atoms aligned in the z-direction.

This Néel state is the obvious choice for $|\Phi\rangle$ in the region $\Delta > 1$ which is known as the Néel-like region. It is convenient to carry out a transformation of the local spin axes at each site on one of the sublattices by performing a rotation of the up-pointing spins by 180° about the y-axis, such that

$$x \to -x, \qquad y \to y, \qquad z \to -z \tag{10.22}$$

and the spin components transform as

$$s^x \to -s^x, \qquad s^y \to s^y, \qquad s^z \to -s^z \tag{10.23}$$

and so

$$s^+ = s^x + is^y \to -s^- \quad \text{and} \quad s^- = s^x - is^y \to -s^+. \tag{10.24}$$

The effect of this transformation is that every spin, whichever sublattice it is on, is now (notionally) pointing 'down' in the Néel state, i.e. with $s^z = -\frac{1}{2}$. This makes the process of determining the CCM equations easier as each site may now be treated equally. The Hamiltonian of Eq. (10.21) in these local coordinates now becomes

$$\mathcal{H} = -\frac{1}{2}\sum_{\langle i,j\rangle}[s_i^+ s_j^+ + s_i^- s_j^- + 2\Delta s_i^z s_j^z]. \tag{10.25}$$

The transformation is canonical and does not alter the commutation relations between the spin operators on a given site. (All spin operators referring to different sites commute). Furthermore, it does not alter the values of the ground-state expectation values or the the excited state energies or spectra. Apart from this 'down' spin state with $s^z = -\frac{1}{2}$, there is only one 'other' state at each site in this new basis, namely, the 'up' state with $s^z = +\frac{1}{2}$. The creation operators used in the CCM ket-state correlation operator S are now clearly always the spin-raising operators s^+. A C_I^+ is a product of these spin-raising operators acting at different sites. (Note that the creation operator cannot act more than once at a given site for a spin-$\frac{1}{2}$ atom, although this restriction would not apply for $s > \frac{1}{2}$.) An example for $s = \frac{1}{2}$ might be $C_I^+ = s_i^+ s_j^+ s_k^+ s_l^+$ in which i, j, k, l are different sites on the lattice.

The transformation is purely a mathematical device, there is no physical rotation of the spins. When considering which other states can be mixed in with the Néel state to form an approximation to the true ground state we must take into account any physical properties we know it must satisfy. In particular, for the Hamiltonian Eq. (10.21) the total z-component of the spins $s_T^z = \sum_i s_i^z$ is a conserved quantity. Since the Néel state has $s_T^z = 0$ we can only mix in states with the same S_T^z and this means that C_I^+ must contain an equal number of spin reversals on each sublattice. Clearly there must be an even number of spin-raising operators, half from each sublattice.

The results presented below are based on the non-localised SUB2 approximation scheme and the localised LSUBm scheme. In the latter we include all *fundamental configurations*, $C_I^+ = s_{k_1}^+, s_{k_2}^+, \cdots s_{k_n}^+$, where the number of contiguous sites is $\leq m$. Fundamental configurations are those which are distinct under the point and space group symmetries of both the lattice and the Hamiltonian. The numbers, N_F and N_{F_e}, of such fundamental configurations for the ground and excited states, respectively, are also further restricted by the use of conservation laws, in particular conservation of s_T^z, as mentioned above. As well as $s_T^z = 0$ for the ground state we have $s_T^z = \pm 1$ for the elementary excited states.

10.3.1 The LSUB2 Approximation for the Spin-Half, Square-Lattice XXZ-Model for the z-Aligned Model State

In the LSUB2 approximation we allow two creation operators and they must be on nearest neighbour sites. The only possible C_I^+, other than C_0^+, are terms of the form $s_l^+ s_{l+\rho_1}^+$ where l is any lattice site and ρ_1 is a vector connecting nearest neighbours. The form of the S operator is thus

$$S = \frac{b_1}{2} \sum_l^N \sum_{\rho_1} s_l^+ s_{l+\rho_1}^+, \tag{10.26}$$

where l runs over all lattice sites and ρ_1 runs over all nearest-neighbour sites to l. Note that b_1 is the sole ket-state correlation coefficient in the LSUB2 approximation scheme.

We now calculate the similarity transforms of the operators in the Hamiltonian, $e^{-S} s_k^\alpha e^S$ for $\alpha = z, +, -$. The commutation relations for the spin operators are given by $[s_l^\pm, s_k^z] = \mp s_k^\pm \delta_{l,k}$ and $[s_l^+, s_k^-] = 2 s_k^z \delta_{l,k}$. Furthermore, the similarity transform may be expanded as a series of nested commutators, given by Eq. (10.8). Hence, we obtain the following explicit forms for these similarity transformed operators

$$\begin{aligned}
\hat{s_i}^+ &= s_i^+ \\
\hat{s_i}^z &= s_i^z + b_1 \sum_{\rho_1} s_i^+ s_{i+\rho_1}^+ \\
\hat{s_i}^- &= s_i^- - 2b_1 \sum_{\rho_1} s_i^z s_{i+\rho_1}^+ - b_1^2 \sum_{\rho_1, \rho_2} s_i^+ s_{i+\rho_1}^+ s_{i+\rho_2}^+.
\end{aligned} \tag{10.27}$$

In each case the otherwise infinite series of operators in the expansion of the similarity transform has terminated to finite order. All of Eq. (10.27) are valid for arbitrary spin, but since we are considering only spin-half systems here for which $(s_i^+)^2|\Phi\rangle = 0$ for *any* lattice site, the term in the third equation in the summations over ρ_1 and ρ_2 for which $\rho_1 = \rho_2$ will be zero. Clearly the similarity transformed version of the Hamiltonian is

$$\hat{\mathcal{H}} = -\frac{1}{2}\sum_{\langle i,j\rangle}[\hat{s}_i^+\hat{s}_j^+ + \hat{s}_i^-\hat{s}_j^- + 2\Delta\hat{s}_i^z\hat{s}_j^z]. \tag{10.28}$$

Note that the sum over $\langle i, j\rangle$ is equivalent to a sum over all sites i and over all nearest neighbours ρ_0, together with a factor of $\frac{1}{2}$ to avoid overcounting, so

$$\hat{\mathcal{H}} = -\frac{1}{4}\sum_i\sum_{\rho_0}[\hat{s}_i^+\hat{s}_{i+\rho_0}^+ + \hat{s}_i^-\hat{s}_{i+\rho_0}^- + 2\Delta\hat{s}_i^z\hat{s}_{i+\rho_0}^z]. \tag{10.29}$$

Substituting the expressions for the spin operators in Eq. (10.27) into the above expression, gives

$$\begin{aligned}\hat{\mathcal{H}} = -\frac{1}{4}\sum_i\sum_{\rho_0}[&s_i^+s_{i+\rho_0}^+ + \{s_i^- - 2b_1\sum_{\rho_1}s_i^zs_{i+\rho_1}^+ - b_1^2\sum_{\rho_1,\rho_2}s_i^+s_{i+\rho_1}^+s_{i+\rho_2}^+\}\times\\ &\{s_{i+\rho_0}^- - 2b_1\sum_{\rho_3}s_{i+\rho_0}^zs_{i+\rho_0+\rho_3}^+ - b_1^2\sum_{\rho_3,\rho_4}s_{i+\rho_0}^+s_{i+\rho_0+\rho_3}^+s_{i+\rho_0+\rho_4}^+\} +\\ &2\Delta\{s_i^z + b_1\sum_{\rho_1}s_i^+s_{i+\rho_1}^+\}\times\{s_{i+\rho_0}^z + b_1\sum_{\rho_2}s_{i+\rho_0}^+s_{i+\rho_0+\rho_2}^+\}].\end{aligned} \tag{10.30}$$

When this $\hat{\mathcal{H}}$ is now used in Eq. (10.13) with $C_I^- = s_m^-s_{m+\rho}^-$ to determine the coefficient b_1, only terms with net two spin-raising operators are needed. When used in Eq. (10.12) for the ground state energy E_g only terms with net zero spin-raising operators are needed. In addition, when calculating the bra state coefficient using Eq. (10.14) terms with net two lowering operators will be needed. Keeping only the terms in Eq. (10.29) with these forms leads to the following simplified expression

$$\hat{\mathcal{H}} \approx \hat{\mathcal{H}}_{-2} + \hat{\mathcal{H}}_0 + \hat{\mathcal{H}}_2$$

where

$$\hat{\mathcal{H}}_{-2} = -\frac{1}{4}\sum_i\sum_{\rho_0}s_i^-s_{i+\rho_0}^-$$

is the part with net two spin lowering operators,

$$\hat{\mathcal{H}}_0 = -\frac{1}{4}\sum_i\sum_{\rho_0}\left[-2b_1\sum_{\rho_3} s_i^- s_{i+\rho_0}^z s_{i+\rho_0+\rho_3}^+ - 2b_1\sum_{\rho_1} s_i^z s_{i+\rho_1}^+ s_{i+\rho_0}^- + 2\Delta s_i^z s_{i+\rho_0}^z\right] \tag{10.31}$$

is the part with net zero spin-raising operators, and

$$\begin{aligned}\hat{\mathcal{H}}_2 = -\frac{1}{4}\sum_i\sum_{\rho_0}\Bigg[& s_i^+ s_{i+\rho_0}^+ + 4b_1^2\sum_{\rho_1,\rho_3} s_i^z s_{i+\rho_1}^+ s_{i+\rho_0}^z s_{i+\rho_0+\rho_3}^+ \\ & - b_1^2\sum_{\rho_3,\rho_4} s_i^- s_{i+\rho_0}^+ s_{i+\rho_0+\rho_3}^+ s_{i+\rho_0+\rho_4}^+ - b_1^2\sum_{\rho_1,\rho_2} s_i^+ s_{i+\rho_1}^+ s_{i+\rho_2}^+ s_{i+\rho_0}^- \\ & + 2\Delta b_1\sum_{\rho_2} s_i^z s_{i+\rho_0}^+ s_{i+\rho_0+\rho_2}^+ + 2\Delta b_1\sum_{\rho_1} s_i^+ s_{i+\rho_1}^+ s_{i+\rho_0}^z\Bigg]\end{aligned} \tag{10.32}$$

is the part with net two spin-raising operators.

First consider Eq. (10.12) for the ground-state energy

$$E_g = \langle\Phi|\hat{\mathcal{H}}|\Phi\rangle = \langle\Phi|\hat{\mathcal{H}}_0|\Phi\rangle.$$

Using the commutator $[s_i^-, s_{i+\rho_0+\rho_3}^+] = -2s_i^z\delta_{i,\,i+\rho_0+\rho_3}$ gives

$$\begin{aligned}\hat{\mathcal{H}}_0 = -\frac{1}{4}\sum_i\sum_{\rho_0}\Bigg[& -2b_1\sum_{\rho_3} s_{i+\rho_0}^z s_{i+\rho_0+\rho_3}^+ s_i^- + 4b_1 s_{i+\rho_0}^z s_i^z \\ & -2b_1\sum_{\rho_1} s_i^z s_{i+\rho_1}^+ s_{i+\rho_0}^- + 2\Delta s_i^z s_{i+\rho_0}^z\Bigg],\end{aligned} \tag{10.33}$$

and when this acts on $|\Phi\rangle$ the terms with a spin lowering operator on the right will give zero. Hence

$$\hat{\mathcal{H}}_0|\Phi\rangle = -\frac{1}{4}\sum_i\sum_{\rho_0}\left[4b_1 s_i^z s_{i+\rho_0}^z + 2\Delta s_i^z s_{i+\rho_0}^z\right]|\Phi\rangle \tag{10.34}$$

$$= -\frac{1}{16}\sum_i\sum_{\rho_0}(4b_1 + 2\Delta)|\Phi\rangle\,. \tag{10.35}$$

since $s_i^z|\Phi\rangle = -\frac{1}{2}|\Phi\rangle$ for all i.
Using Eq. (10.12), the ground-state energy is

$$\frac{E_g}{N} = -\frac{n}{8}(\Delta + 2b_1). \tag{10.36}$$

where n is the number of nearest neighbours.

Equation (10.36) shows that the ground-state energy is size-extensive (i.e., it scales linearly with N), as required by the Goldstone theorem which is obeyed by the NCCM. In fact it is easy to show that *any* other non-trivial choice for S, not just the LSUB2 approximation, will always yield expression (10.36) for the ground-state energy, although the calculation of b_1 will be different. The task is therefore to find b_1. If we could include all possible spin correlations in S then we would obtain an exact result for b_1 and hence the ground-state energy. This is of course impossible except for trivial cases so there will normally need to be an approximation like the ones described here.

In this LSUB2 approximation b_1 is the only non-zero coefficient in S and it is determined using $\hat{\mathcal{H}}_2$ in Eq. (10.13), with $C_I^- = s_m^- s_{m+\rho}^-$

$$\langle \Phi | C_I^- \hat{\mathcal{H}} | \Phi \rangle = \langle \Phi | C_I^- \hat{\mathcal{H}}_2 | \Phi \rangle = 0 . \tag{10.37}$$

since C_I^- has two lowering operators. The details of the calculation are given in the appendix where it is shown that Eq. (10.37) yields

$$(n+1)b_1^2 + 2(n-1)\Delta b_1 - 1 = 0. \tag{10.38}$$

Equations (10.36) and (10.38) are the basic equations in the LSUB2 approximation for the linear chain with $n = 2$, the square lattice with $n = 4$ and the cubic lattices. Similar results can be obtained for any other bipartite lattice with nearest-neighbour interactions.

For the linear chain these equations become

$$\frac{E_g}{N} = -\frac{1}{4}(\Delta + 2b_1) \quad \text{with} \quad 3b_1^2 + 2\Delta b_1 - 1 = 0, \tag{10.39}$$

so that

$$b_1 = \frac{1}{3}(\sqrt{\Delta^2 + 3} - \Delta) \quad \text{and} \quad \frac{E_g}{N} = -\frac{\Delta}{12} - \frac{\sqrt{\Delta^2 + 3}}{6} . \tag{10.40}$$

This gives a value for ground-state energy the isotropic Heisenberg model ($\Delta = 1$) of $\frac{E_g}{N} = -\frac{5}{12} (\equiv -0.416667)$ (to 6 decimal places), which compares to the exact result of $\frac{E_g}{N} = -0.443147J$ (again to 6 decimal places). This is an improvement on energy of the (classical) model state, which is $\frac{E_g}{N} = -\frac{1}{4}$.
However, we shall consider only the square lattice with $n = 4$ from now on, for which

$$\frac{E_g}{N} = -\frac{1}{2}(\Delta + 2b_1) \quad \text{with} \quad 5b_1^2 + 6\Delta b_1 - 1 = 0, \tag{10.41}$$

so that

$$b_1 \;=\; \frac{1}{5}(\sqrt{9\Delta^2+5}-3\Delta) \quad \text{and} \quad \frac{E_g}{N} \;=\; \frac{\Delta}{10}-\frac{1}{5}\sqrt{9\Delta^2+5}\,. \tag{10.42}$$

This expression gives the correct result in the Ising limit $\Delta \to \infty$. These results for the ground-state energy as a function of Δ in the LSUB2 approximation are included in both Figs. 10.1 and 10.2.

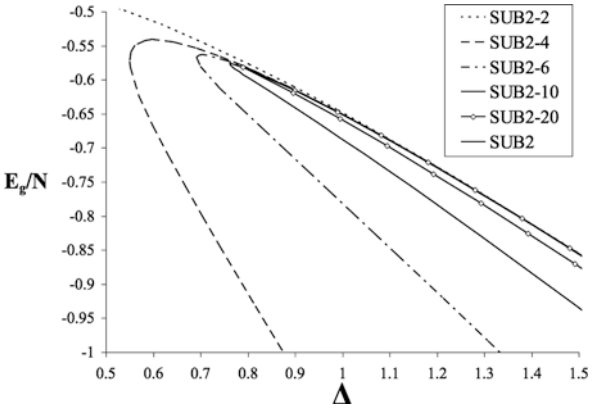

Fig. 10.1 CCM SUB2-m and SUB2 results using the z-aligned Néel model state for the ground-state energy of the spin-half square-lattice XXZ-Model. (Note that SUB2-2 and LSUB2 are equivalent approximations)

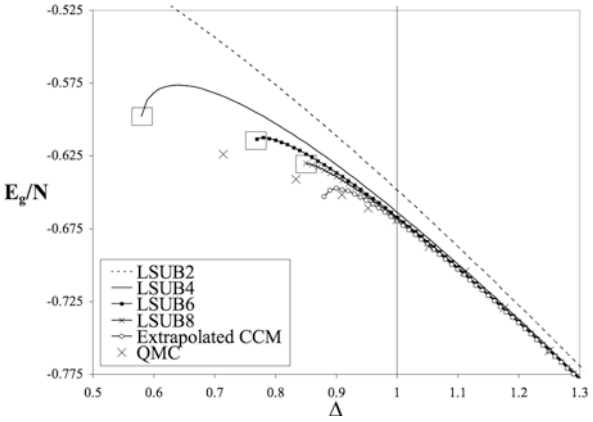

Fig. 10.2 CCM LSUBm results for the ground-state energy of the spin-half square-lattice XXZ-Model compared to quantum Monte Carlo results of Barnes et al. [12]

A similar calculation, based on Eq. (10.14) although not using it directly, gives the following equation for $\tilde{b}_1$. Again details are given in the appendix.

$$\tilde{b}_1[(n+1)2b_1+2(n-1)\Delta]-1 \;=\; 0. \tag{10.43}$$

For the square lattice with $n = 4$ this becomes

$$10b_1\tilde{b}_1 + 6\Delta\tilde{b}_1 - 1 \;=\; 0, \tag{10.44}$$

which gives $\tilde{b}_1 = \frac{1}{2}(9\Delta^2 + 5)^{-1/2}$.

Finally, we note that once the values for the bra- and ket-state correlation coefficients have been determined (at a given level of approximation) then we can also evaluate various expectation values. An important example is the sublattice magnetisation given by

$$M \equiv \frac{2}{N}\langle\tilde{\Psi}|\sum_i^N(-1)^i s_i^z|\Psi\rangle, \tag{10.45}$$

in terms of the original unrotated spin coordinates. After rotation of the local spin axes

$$M \;=\; -\frac{2}{N}\langle\tilde{\Psi}|\sum_i^N s_i^z|\Psi\rangle \;=\; -\frac{2}{N}\langle\Phi|\tilde{S}e^{-S}\left(\sum_i^N s_i^z\right)e^S|\Phi\rangle, \tag{10.46}$$

in terms of the 'rotated' spin coordinates. For the square lattice in the LSUB2 approximation this is given by

$$\begin{aligned} M_{\mathrm{LSUB2}} &= 1 - 8b_1\tilde{b}_1, \\ &= \frac{1}{5}\left[1 + \frac{12\Delta}{\sqrt{9\Delta^2+5}}\right]. \end{aligned} \tag{10.47}$$

This result is shown in Fig. 10.3.

10.3.2 The SUB2 Approximation for the Spin-Half, Square-Lattice XXZ-Model of the z-Aligned Model State

The LSUB2 approximation is the simplest possible, including in S terms with just two spin flips which have to be on adjacent sites. Of course the exponentiation of the S operator, e^S, results in multiple applications of this and so the approximate ground state calculated in the previous section includes contributions from states with arbitrarily large numbers of flips at widely separated sites.

The SUB2 approximation is a generalisation of this in which all possible two-spin-flip terms are included in S. These can now be at any two sites although, of course one must be on one sublattice and the other on the other sublattice. The SUB2 ket-state operator S is given by

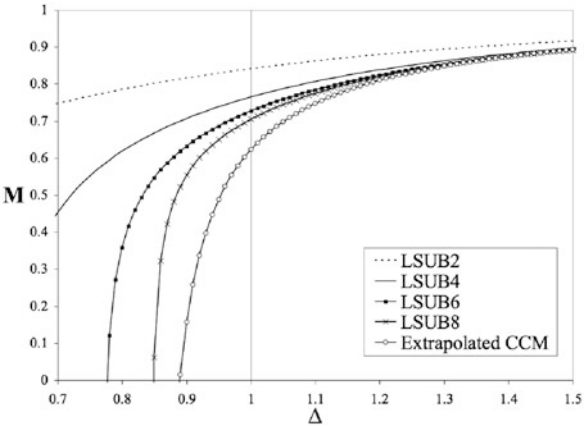

Fig. 10.3 CCM LSUBm results using the z-aligned Néel model states for the sublattice magnetisation of the spin-half square-lattice XXZ-Model

$$S = 1/2 \sum_{i}^{N} \sum_{r} b_r s_i^+ s_{i+r}^+, \tag{10.48}$$

where the index i runs over all sites on the lattice chain. The index r runs over all lattice vectors which connect one sublattice to the other and b_r is the corresponding SUB2 ket-state correlation coefficient for this vector. The similarity transformed versions of the operators are

$$\begin{aligned} \tilde{s}_l^+ &= s_l^+ \\ \tilde{s}_l^z &= s_l^z + \sum_r b_r s_l^+ s_{l+r}^+ \\ \tilde{s}_l^- &= s_l^- - 2\sum_r b_r s_l^z s_{l+r}^+ - \underbrace{\sum_{r_1, r_2}}_{r_1 \neq r_2} b_{r_1} b_{r_2} s_l^+ s_{l+r_1}^+ s_{l+r_2}^+. \end{aligned} \tag{10.49}$$

Again we note that $(s_i^+)^2|\Phi\rangle = 0$ for *any* lattice site (which is true only for spin-half systems). Hence, we see that $r_1 \neq r_2$ in the above equations. We now substitute these expressions into Eq. (10.25) in order to obtain $\tilde{\mathcal{H}}$, and we then use Eq. (10.13) in order to obtain the following equation for the correlation coefficients $\{b_r\}$

$$\sum_{\rho} \left\{ (1 + 2\Delta b_1 + 2b_1^2)\delta_{\rho,r} - 2(\Delta + 2b_1)b_r + \sum_s b_{r-s-\rho_1} b_{s+\rho+\rho_1} \right\} = 0, \tag{10.50}$$

where ρ runs over all nearest-neighbour vectors on the square lattice and ρ_1 is any one of them. Equation (10.50) may now be solved using a sublattice Fourier transform, given by

$$\Gamma(q) = \sum_r e^{\mathbf{ir}.\mathbf{q}} b_r, \tag{10.51}$$

where the sum over r is a sum over the position vectors of *one* sublattice only. A convenient way to achieve this for the two-dimensional square lattice is to require that $r_x + r_y$ is an odd integer number. This expression has an inverse given by

$$b_r = \int_{-\pi}^{\pi} \int_{-\pi}^{\pi} \frac{dq_y dq_x}{(2\pi)^2} \cos(r_x q_x) \cos(r_y q_y) \Gamma(q). \tag{10.52}$$

The SUB2 Eqs. (10.50) and (10.51) lead to the following expression [5] for $\Gamma(q)$

$$\Gamma(q) = \frac{K}{\gamma(q)} \left[1 \pm \sqrt{1 - k^2 \gamma^2(q)} \right], \tag{10.53}$$

$$K = \Delta + 2b_1, \quad k^2 = (1 + 2\Delta b_1 + 2b_1^2)/K^2 \text{ and}$$

$$\gamma(q) = \frac{1}{n} \sum_{\rho} e^{i\rho.\mathbf{q}} \left(\equiv \frac{1}{2} \{\cos(q_x) + \cos(q_y)\} \text{ for the square lattice} \right) \tag{10.54}$$

(Note that we choose the negative solution in Eq. (10.53) such that the result is correct in the trivial limit $\Delta \to \infty$.) Equations (10.52), (10.53) and (10.54) lead to a self-consistency requirement on the variable b_1 and they may be solved iteratively at a given value of Δ. Indeed, we know that all correlation coefficients must tend to zero (namely, for SUB2: $b_r \to 0, \ \forall\, r$) as $\Delta \to \infty$ and we *track* this solution for large Δ by reducing Δ in small successive steps. We find that the discriminant in Eq. (10.53) becomes negative at a *critical point*, $\Delta_c \approx 0.7985$. This is an indication that the CCM critical point corresponds to a quantum phase transition in the system, although in this simple approximation scheme it is some way from the known phase transition at $\Delta = 1$.

We may also solve the SUB2-*m* equations directly using computational techniques. (Note that the SUB2-2 and LSUB2 approximations are equivalent.) Indeed, we study the limit points of these coupled non-linear equations may be obtained with respect to Δ. We again track our solution from the limit $\Delta \to \infty$ to (and beyond) the limit point and Fig. 10.1 shows our results. In particular, we note that we have two distinct branches, although only the upper branch is a 'physical' solution. We have already remarked that the CCM does not necessarily always provide an upper bound on the ground-state energy, although this is often the case for the 'physical' solution. An example of this is seen by the 'unphysical' lower branch in Fig. 10.1. However, the solution of the CCM equations will often naturally converge to the physical solution, provided we have a reasonable starting point for the CCM correlation coefficients and our model state is also reasonable. However, by tracking from a point at which we are sure of (in this case, from the limit $\Delta \to \infty$), we ensure that our solution is indeed the correct one. This approach is also used for LSUB*m* approximations.

We see in Fig. 10.1 that the two branches collapse onto the same line (namely, that of the full SUB2 solution) as we increase the level of SUB2-m approximation with respect to m. Indeed, we may plot the positions of the SUB2-m limit points against $1/m^2$ and we note that these data points are found to be both highly linear and they tend to the critical value, Δ_c, of the full SUB2 equations in the limit $m \to \infty$. Again, we note that the LSUBm and SUBm-m a approximations also show similar branches (namely, one 'physical' and one 'unphysical' branch) which appear to converge as one increases the magnitude of the truncation index, m, although results for the 'unphysical' branches are not presented here for the LSUBm approximation. This is a strong indication that our LSUBm and SUBm-m critical points are also reflections of phase transitions in the real system. We expect that our extrapolated LSUBm and SUBm-m critical points should tend to the exact solution.

10.3.3 High-Order CCM Calculations Using a Computational Approach

We now consider the localised LSUBm and SUBm-m approximation schemes for larger values of m than $m = 2$. Recall that LSUBm allows all possible terms in S in which spin flips all occur within a *locale* of size m. For spin-half the maximum number of spin-raising operators in one term is m, but for general spin quantum number, s, it is $2sm$. SUBm-n is a scheme in which one allows a maximum of m spin-raising operators in any one term and restricts them to all lie within a locale of size n. This locale is defined by those configurations that contain m contiguous sites. For spin-half systems, SUBm-m is the same as LSUBm and this is the only type considered here. These schemes are more complicated and cannot usually be treated analytically as we were able to do for LSUB2 and SUB2. Consequently, computational techniques are used both to determine the CCM equations and then to solve them numerically.

There are two methods of doing this. Firstly, one may use computer algebraic methods to calculate the similarity transformed versions of the individual spin operators and hence the similarity transformed version of the Hamiltonian, which may involve further commutations of the spin operators. This approach has the advantage of flexibility and can be applied to any Hamiltonian in principle. Often, however, this method is somewhat cumbersome and slow.

A second method is to first cast the CCM ket-state correlation operator into a form given by

$$S = \sum_{i_1}^{N} \mathcal{S}_{i_1} s_{i_1}^{+} + \sum_{i_1,i_2} \mathcal{S}_{i_1,i_2} s_{i_1}^{+} s_{i_2}^{+} + \cdots \tag{10.55}$$

with respect to a model state in which all spins point in the downwards z-direction. Here the $\mathcal{S}_{i_1,\cdots,i_l}$ represent the CCM ket-state correlation coefficients

as in Eq. (10.5). We now define new operators given by

$$F_k = \sum_{l} \sum_{i_2,\cdots,i_l} l\mathcal{S}_{k,i_2,\cdots,i_l} s^+_{i_2} \cdots s^+_{i_l}$$
$$G_{k,m} = \sum_{l>1} \sum_{i_3,\cdots,i_l} l(l-1)\mathcal{S}_{k,m,i_3,\cdots,i_l} s^+_{i_3} \cdots s^+_{i_l} \tag{10.56}$$

for the spin-half quantum spin systems. (For $s > 1/2$ additional terms are needed). For the spin-half system the similarity transformed operators can be written

$$\begin{aligned} \tilde{s}^+_k &= s^+_k \\ \tilde{s}^z_k &= s^z_k + F_k s^+_k \\ \tilde{s}^-_k &= s^-_k - 2F_k s^z - (F_k)^2 s^+_k . \end{aligned} \tag{10.57}$$

These expressions can now be substituted analytically into the (similarity transformed) Hamiltonian and the commutations evaluated by hand. The Hamiltonian is then written in terms of these new operators of Eq. (10.56), which are themselves made up purely of spin-raising operators.

This second method requires more direct effort in setting up the Hamiltonian in terms of these new operators, compared to the first method in which computer algebraic techniques are used to take care of this aspect. However, once this is accomplished, the problem of finding the ket-state equations reduces to pattern matching of our target fundamental configurations to those terms in the Hamiltonian. This form is well suited to a computational implementation because no further commutations or re-ordering of terms in the Hamiltonian is necessary. The bra-state equations may also be directly determined once the ground-state energy and CCM ket-state equations have been determined.

Results for the ground-state energy of the spin-half square-lattice XXZ-Model are shown in Fig. 10.2 and for the spin-half Heisenberg model ($\Delta = 1$) in Table 10.1. We note that good correspondence with the results of quantum Monte Carlo (QMC) [12] are observed. The extrapolated value for the CCM ground-state energy of $E_g/N = -0.6696$ compares well with results of QMC [13] that give $E_g/N = -0.669437(5)$. We see clearly from Fig. 10.2 that the results based on the (z-aligned) model state rapidly converge with increasing level of LSUBm approximation in the region $\Delta \geq 1$. CCM results compare well to results of QMC [12] for $\Delta \geq 1$ based on this model state. Results for the sublattice magnetisation using the LSUBm approximation are shown in Fig. 10.3 and for the spin-half Heisenberg model ($\Delta = 1$) in Table 10.1. We see again that LSUBm results converge rapidly with increasing level of approximation in the region $\Delta \geq 1$. We see that the extrapolated CCM result of $M = 0.614$ again compares well to QMC results [13] of $M = 0.6140(6)$. Results for the CCM critical points are also shown in Table 10.1. We see that the values for the critical points, Δ_c, extrapolate [7] to a value close to $\Delta = 1$, at (or near to) which point a quantum phase transition is believed to occur.

Table 10.1 CCM results [7] for the isotropic ($\Delta = 1$) spin-half square-lattice Heisenberg antiferromagnet compared to results of other methods. The numbers of fundamental configurations in the ground-state and excited-state CCM wave functions for the z-aligned Néel model state are given by N_f^z and N_{fe}^z, respectively. Results for the critical points of the z-aligned Néel model state are indicated by Δ_c. (We note LSUB2 never terminates and so there is no value for Δ_c, and this is indicated by the symbol '–'.) Details of extrapolation procedures are presented in [7]. CCM results for the spin-stiffness ρ are from [10]. Results for the magnetic susceptibility χ are determined via $\chi = \frac{dM^L}{d\lambda}$. Those results that have not, as yet, been determined at a given level of approximation have been left blank

Method	E_g/N	M	ε_e	ρ	χ	N_f^z	N_{fe}^z	Δ_c
LSUB2	−0.64833	0.841	1.407	0.2310	0.0860	1	1	–
SUB2	−0.65083	0.827	1.178			∞	∞	0.799
LSUB4	−0.66366	0.765	0.852	0.2310	0.0792	7	6	0.577
LSUB6	−0.66700	0.727	0.610	0.2176	0.0765	75	91	0.763
LSUB8	−0.66817	0.705	0.473	0.2097	0.0750	1,273	2,011	0.843
LSUB10	−0.668700	0.345			0.0739	29,605	51,012	
LSUB12	−0.668978	0.339				766,220		
Extrapolated CCM	−0.66960	0.614	0.00	0.1812	0.070	∞	∞	1.03

Finally, results for the spin stiffness of the spin-half square-lattice Heisenberg model may be determined [10], and these results are also shown in Table 10.1. Again, the extrapolated value $\rho = 0.1812$ from Krüger et al. [10] compares well to the corresponding result of QMC [14] of $\rho = 0.199$.

10.3.4 Excitation Spectrum of the Spin-Half Square-Lattice XXZ-Model for the z-Aligned Model State

We now consider the excitation spectrum. We shall use the SUB2 approximation for the ground state, whereas for the excitation operator we assume

$$X = \sum_i a_i s_i^+. \tag{10.58}$$

Substitution of the expressions in Eqs. (10.48) and (10.58) for the ground- and excited-state operators, respectively, leads to the following expression [5] for the excited-state correlation coefficients

$$\frac{1}{2}nKa_k - \frac{1}{2}\sum_{\rho,r} b_r a_{k+r+\rho} = \varepsilon_e a_k. \tag{10.59}$$

This equation may also be solved by Fourier transform techniques in a similar manner presented above for the SUB2 calculation for the ground state. The result of this treatment is an expression for the excitation spectra is given by

$$\varepsilon(q) = \frac{1}{2} nK\sqrt{1 - k^2\gamma^2(q)}, \tag{10.60}$$

where b_1 is obtained from the SUB2 ket-state equations and K and k are defined by Eq. (10.54). We solve the SUB2 equations as normal at a particular value of Δ and then b_1 is substituted into Eq. (10.60) above and hence we obtain values for the excitation spectra as a function of the wave vector Eq. (10.60). Note that the excitation spectra becomes 'soft' (i.e. $\varepsilon(q) \to 0$) at the CCM SUB2 critical point at $\Delta_c \approx 0.7985$ as mentioned earlier. Results for the spectra are presented in Fig. 10.4). We see that the CCM results are in good agreement with those results of linear spin-wave theory at $\Delta = 1$. The spectra are plotted for $k_x = k_y$ and for $k_y = 0$, and we see that the CCM excitation spectrum is identical in shape to those results of SWT with a multiplicative factor of 1.1672. This agrees well with results of quantum Monte Carlo [15] that also predict a curve identical to SWT with multiplicative a factor of 1.21±0.03. Our results in thus in good agreement with SWT and QMC and this is further evidence that the CCM critical point is an indication of the quantum phase transition at $\Delta = 1$ in the 'real' system. Furthermore, the excitation spectra at this point is given by $\varepsilon(q) = \frac{1}{2} nK\sqrt{1 - \gamma^2(q)}$. This leads to a value for the spin-wave velocity v_s of $\frac{1}{2} nK$, which in turn yields a value [5] of $v_s \approx 2.335$ for the square-lattice case.

Finally, it is worth mentioning that the excitation energy may be determined directly from Eq. (10.20) in 'real space' without recourse to Fourier transform methods, although computational techniques are again necessary except for the simplest of cases. For the sake of consistency, we normally retain the same level of localised approximation for the ground and excited states. Results are presented for the XXZ-Model in Fig. 10.5 and for the Heisenberg model in Table 10.1. For the latter we see that the CCM results converge rapidly with LSUBm approximation level. Indeed, extrapolated results predict that the excitation is gapless at $\Delta = 1$,

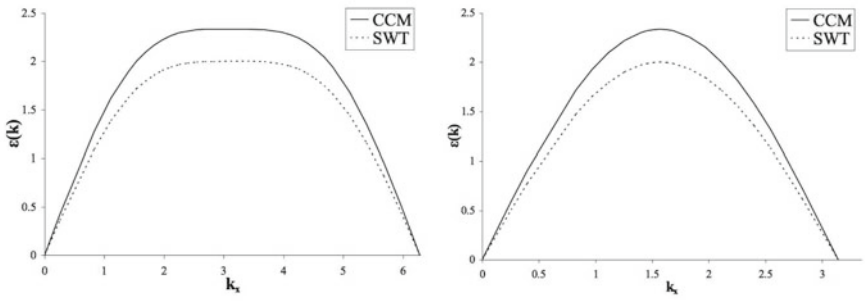

Fig. 10.4 Excitation spectra for the Heisenberg model determined at the critical point at $\Delta_c = 0.8$ for the CCM results and at $\Delta = 1$ for the spin-wave theory results. The spectra plotted on the left are for $k_x = k_y$ and those on the right are for $k_y = 0$. This agrees well with results of quantum Monte Carlo [15] that also predict a curve identical to SWT with a multiplicative factor of 1.21±0.03, respectively

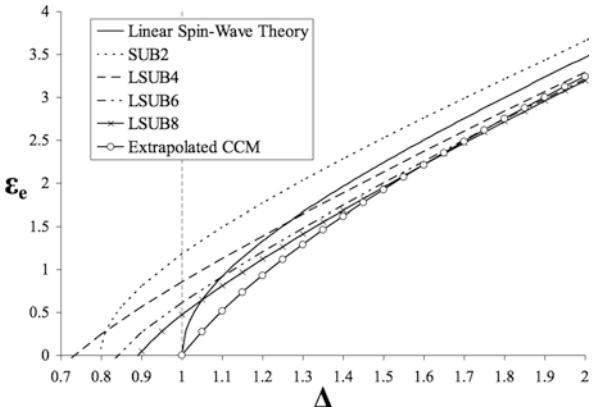

Fig. 10.5 CCM LSUBm results using the z-aligned Néel model state for the excited-state energy of the spin-half square-lattice XXZ-Model compared to linear spin-wave theory of Barnes et al. [12]

as is believed to be the case for the Heisenberg model from the results of other approximate calculations.

10.4 The Lattice Magnetisation

The lattice magnetisation is a quantity that yields an overall response of a particular quantum spin system as a whole to the externally applied magnetic field. The lattice magnetisation gives the average ordering of the spins in the direction of the externally applied magnetic field and it is defined by the equation

$$M^L \equiv -\frac{2}{N}\langle\tilde{\Psi}|\sum_i^N s_i^z|\Psi\rangle, \tag{10.61}$$

in terms of the original unrotated spin coordinates. In terms of the rotated spin coordinates, an additional factor of $(-1)^i$ is also included in Eq. (10.61). The relevant Hamiltonian for the Heisenberg model is defined by

$$\mathcal{H} = \sum_{\langle i,j\rangle} \mathbf{s}_i \cdot \mathbf{s}_j - \lambda \sum_i s_i^z \ , \tag{10.62}$$

where the indices i and j again run over all nearest-neighbouring lattice sites on the square lattice, although counting each bond once only, and λ indicates the strength of the external field. We must also take into account the fact that spins in the model state are explicitly allowed to cant at an angle θ to the negative and positive x-axes for the difference sublattices. This angle is treated a parameter that we treat variationally in order to obtain the best results for the energy. The total

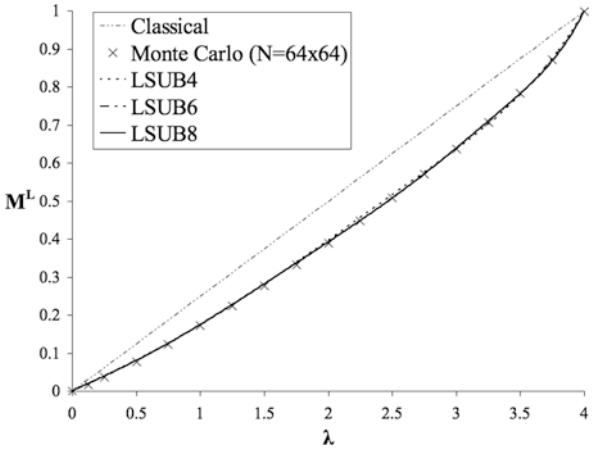

Fig. 10.6 Results for the lattice magnetisation of the spin-half square-lattice Heisenberg model in the presence of an external magnetic field of strength λ compared to results of quantum Monte Carlo [16] for $N = 64 \times 64$ and classical results

lattice magnetisation may be determined directly in a similar manner as presented above for the sublattice magnetisation. The results for the spin-half square-lattice Heisenberg model are shown in Fig. 10.6. As for the ground and excited-state energies and the sublattice magnetisations, we obtain results that converge rapidly with increasing levels of LSUBm approximation and that compare well to the results of QMC for $N = 64 \times 64$. The magnetic susceptibility may also be determined via $\chi = \frac{dM^L}{d\lambda}$ and results are shown in Table 10.1. The extrapolated CCM values of $\chi = 0.070$ for $\lambda \to 0$ again compares reasonably well to the result of QMC [17] of $\chi = 0.0669(7)$. The zero-field uniform susceptibility ($\lambda \to 0$), the ground state energy, the sublattice magnetisation, the spin stiffness, and the spin-wave velocity constitute the fundamental parameter set that determines the low-energy physics of magnetic systems. The CCM is thus able to provide a comprehensive and accurate picture of the properties of spin-half square-lattice Heisenberg model.

Appendix – Details of the Calculation of the Coefficients b_1 and $\tilde{b_1}$ in the LSUB2 Approximation

The first step in simplifying the expression for $\hat{\mathcal{H}}_2$ is to move all s^- and s^z operators to the right, using the commutation relations, noting that i and $i + \rho_0$ are on different sublattices and cannot be equal, whereas i and $i + \rho_0 + \rho_1$ are on the same sublattice, etc.

$$\begin{aligned}\hat{\mathcal{H}}_2 \;=\; & -\frac{1}{4}\sum_i\sum_{\rho_0}\Bigg[s_i^+ s_{i+\rho_0}^+ + 4b_1^2\sum_{\rho_1,\ \rho_3} s_{i+\rho_1}^+ s_{i+\rho_0+\rho_3}^+ s_i^z s_{i+\rho_0}^z \\ & + 4b_1^2\sum_{\rho_1} s_{i+\rho_1}^+ s_i^+ s_{i+\rho_0}^z - b_1^2\sum_{\rho_3,\ \rho_4} s_{i+\rho_0}^+ s_{i+\rho_0+\rho_3}^+ s_{i+\rho_0+\rho_4}^+ s_i^- \\ & + 2b_1^2\sum_{\rho_3} s_{i+\rho_0}^+ s_{i+\rho_0+\rho_3}^+ s_i^z + 2b_1^2\sum_{\rho_4} s_{i+\rho_0}^+ s_{i+\rho_0+\rho_4}^+ s_i^z + 2b_1^2 s_i^+ s_{i+\rho_0}^+ \\ & - b_1^2\sum_{\rho_1,\ \rho_2} s_i^+ s_{i+\rho_1}^+ s_{i+\rho_2}^+ s_{i+\rho_0}^- + 2\Delta b_1\sum_{\rho_2} s_{i+\rho_0}^+ s_{i+\rho_0+\rho_2}^+ s_i^z \\ & + 2\Delta b_1 s_i^+ s_{i+\rho_0}^+ + 2\Delta b_1\sum_{\rho_1} s_i^+ s_{i+\rho_1}^+ s_{i+\rho_0}^z\Bigg]\end{aligned}$$

The terms with s^- on the right will give zero when acting on $|\Phi\rangle$ so after simplifying the subscripts

$$\begin{aligned}\hat{\mathcal{H}}_2|\Phi\rangle \;=\; & -\frac{1}{4}\sum_i\sum_{\rho_0}\Bigg[s_i^+ s_{i+\rho_0}^+ + 4b_1^2\sum_{\rho_1,\ \rho_3} s_{i+\rho_1}^+ s_{i+\rho_0+\rho_3}^+ s_i^z s_{i+\rho_0}^z \\ & + 4b_1^2\sum_{\rho_1} s_{i+\rho_1}^+ s_i^+ s_{i+\rho_0}^z \;+ 4b_1^2\sum_{\rho_1} s_{i+\rho_0}^+ s_{i+\rho_0+\rho_1}^+ s_i^z \\ & + 2b_1^2 s_i^+ s_{i+\rho_0}^+ + 2\Delta b_1\sum_{\rho_2} s_{i+\rho_0}^+ s_{i+\rho_0+\rho_2}^+ s_i^z \\ & + 2\Delta b_1 s_i^+ s_{i+\rho_0}^+ + 2\Delta b_1\sum_{\rho_1} s_i^+ s_{i+\rho_1}^+ s_{i+\rho_0}^z\Bigg]|\Phi\rangle\,.\end{aligned}$$

Also $s_i^z|\Phi\rangle \;=\; -\frac{1}{2}|\Phi\rangle$ for all i so

$$\begin{aligned}\hat{\mathcal{H}}_2|\Phi\rangle \;=\; & -\frac{1}{4}\sum_i\sum_{\rho_0}\Bigg[s_i^+ s_{i+\rho_0}^+ + b_1^2\sum_{\rho_1,\ \rho_3} s_{i+\rho_1}^+ s_{i+\rho_0+\rho_3}^+ \\ & - 2b_1^2\sum_{\rho_1} s_{i+\rho_1}^+ s_i^+ \;- 2b_1^2\sum_{\rho_1} s_{i+\rho_0}^+ s_{i+\rho_0+\rho_1}^+ + 2b_1^2 s_i^+ s_{i+\rho_0}^+ \\ & - \Delta b_1\sum_{\rho_2} s_{i+\rho_0}^+ s_{i+\rho_0+\rho_2}^+ + 2\Delta b_1 s_i^+ s_{i+\rho_0}^+ - \Delta b_1\sum_{\rho_1} s_i^+ s_{i+\rho_1}^+\Bigg]|\Phi\rangle\,.\end{aligned} \tag{10.63}$$

This is now substituted into Eq. (10.37) which is evaluated making use of the following

1.

$$\langle\Phi|s_i^- s_j^+|\Phi\rangle \;=\; \langle\Phi|(-2s_i^z)|\Phi\rangle\delta_{ij} \;=\; \langle\Phi|\Phi\rangle\delta_{ij} \;=\; \delta_{ij},$$

2. In the following we assume that $m \neq m'$. Typically m and m' are on different sublattices although not necessarily nearest neighbours.

$$\begin{aligned}\langle\Phi|s_l^- s_{l'}^- s_m^+ s_{m'}^+|\Phi\rangle &= \langle\Phi|s_l^- s_m^+ s_{l'}^- s_{m'}^+|\Phi\rangle + \langle\Phi|s_l^-(-2s_m^z)s_{m'}^+|\Phi\rangle\delta(l'-m)\\ = \langle\Phi|s_l^- s_m^+ s_{m'}^+ s_{l'}^-|\Phi\rangle &+ \langle\Phi|s_l^- s_m^+(-2s_{m'}^z)|\Phi\rangle\delta(l'-m') + \langle\Phi|s_l^- s_{m'}^+|\Phi\rangle\delta(l'-m)\\ &= \langle\Phi|s_l^- s_m^+|\Phi\rangle\delta(l'-m') + \langle\Phi|s_l^- s_{m'}^+|\Phi\rangle\delta(l'-m)\\ &= \delta(l-m)\delta(l'-m') + \delta(l-m')\delta(l'-m)\end{aligned}$$

where $\delta(i-j) \equiv \delta_{i-j,\,0} = \delta_{ij}$.

In particular we the following two special cases of this result

$$\begin{aligned}\langle\Phi|s_l^- s_{l+\rho'}^- s_m^+ s_{m+\rho}^+|\Phi\rangle &= \delta(l-m)\delta(l+\rho'-m-\rho)+\delta(l-m-\rho)\delta(l+\rho'-m)\\ &= \delta(l-m)\delta(\rho'-\rho) + \delta(l-m-\rho)\delta(\rho+\rho')\end{aligned}$$

and

$$\begin{aligned}\langle\Phi|s_l^- s_{l+\rho'}^- s_{m+\rho_0+\rho_3}^+ s_{m+\rho}^+|\Phi\rangle &= \delta(l-m-\rho_0-\rho_3)\delta(l+\rho'-m-\rho)+\\ &\qquad \delta(l-m-\rho)\delta(l+\rho'-m-\rho_0-\rho_3)\\ &= \delta(l-m)\delta(\rho_0+\rho_3+\rho'-\rho)+\\ &\qquad \delta(l-m-\rho)\delta(\rho+\rho'-\rho_0-\rho_3)\end{aligned}$$

3.

$$\sum_{\rho_1}\delta(\rho+\rho_1) = 1$$

since there is just one ρ_1 equal to $-\rho$.

4. For the linear chain, the square lattice and the simple cubic

$$\sum_{\rho_1,\rho_2,\rho_3}\delta(\rho+\rho_1+\rho_2+\rho_3) = 3n-3$$

where n is the number of nearest neighbours, this being the number of ways that $\rho_1+\rho_2+\rho_3$ can be made equal to $-\rho$.

In (10.37) we need

$$\langle\Phi|C_I^-\hat{\mathcal{H}}_2|\Phi\rangle = \langle\Phi|s_m^- s_{m+\rho}^-\hat{\mathcal{H}}_2|\Phi\rangle$$

and using the above results and (10.63)

$$\begin{aligned}&= -\frac{1}{4}[2+2b_1^2(3n-3)-4b_1^2 n-4b_1^2 n+4b_1^2\\ &\qquad -\Delta b_1 2n+4\Delta b_1-\Delta b_1 2n] = 0\\ &= -\frac{1}{2}[1-(n+1)b_1^2+2(1-n)\Delta b_1] = 0\end{aligned}$$

which yields Eq. (10.38):

$$(n+1)b_1^2 + 2(n-1)\Delta b_1 - 1 \;=\; 0.$$

We now turn to the bra state and recall that it is not, in general, the Hermitian conjugate of the ket state. In the LSUB2 approximation, which keeps only nearest-neighbour correlations, the operator $\tilde{S}$ has the form

$$\tilde{S} \;=\; 1 + \frac{\tilde{b}_1}{2} \sum_{l}^{N} \sum_{\rho'} s_l^- s_{l+\rho'}^-, \tag{10.64}$$

where the index l runs over all sites on the lattice, ρ' runs over all nearest-neighbour sites, and $\tilde{b}_1$ is the sole bra-state correlation coefficient. $\tilde{b}_1$ can be determined using Eq. (10.14) with $C_I^+ \;=\; s_m^+ s_{m+\rho}^+$. However, it is much quicker to use a shortcut, which we show here only for the LSUB2 version.

First note that $\hat{s_i}^+ \;=\; s_i^+$ so that $\hat{C}_I^+ \;=\; C_I^+$ and Eq. (10.14) becomes

$$\begin{aligned}
\langle \Phi |\, \tilde{S}[\hat{\mathcal{H}}, C_I^+]\, | \Phi \rangle \;&=\; 0 \\
\langle \Phi |\, \tilde{S}[\hat{\mathcal{H}}, s_m^+ s_{m+\rho}^+]\, | \Phi \rangle \;&=\; 0 \\
\therefore \quad b_1 \sum_m \sum_\rho \langle \Phi |\, \tilde{S}[\hat{\mathcal{H}}, s_m^+ s_{m+\rho}^+]\, | \Phi \rangle \;&=\; 0 \\
\therefore \quad \langle \Phi |\, \tilde{S}[\hat{\mathcal{H}}, S]\, | \Phi \rangle \;&=\; 0
\end{aligned} \tag{10.65}$$

since $S \;=\; b_1 \sum_m \sum_\rho s_m^+ s_{m+\rho}^+$.

Now consider

$$\begin{aligned}
\frac{\partial \bar{\mathcal{H}}}{\partial b_1} \;&=\; \frac{\partial}{\partial b_1} \langle \Phi | \tilde{S} e^{-S} \mathcal{H} e^{S} | \Phi \rangle \\
&=\; \langle \Phi | \left\{ \tilde{S} \left(-e^{-S} \frac{\partial S}{\partial b_1} \right) \mathcal{H} e^{S} + e^{-S} \mathcal{H} \left(e^{S} \frac{\partial S}{\partial b_1} \right) \right\} | \Phi \rangle
\end{aligned}$$

since b_1 occurs only in S and not in $\tilde{S}$ or $\mathcal{H}$.

Also since $S \;=\; b_1 \sum_m \sum_\rho s_m^+ s_{m+\rho}^+$, it follows that $\dfrac{\partial S}{\partial b_1} \;=\; \dfrac{1}{b_1} S$ so

$$\frac{\partial \bar{\mathcal{H}}}{\partial b_1} \;=\; \frac{1}{b_1} \langle \Phi |\, \tilde{S}[\hat{\mathcal{H}}, S]\, | \Phi \rangle \;=\; 0$$

because of Eq. (10.65). Thus it is sufficient to evaluate $\bar{\mathcal{H}}$ and differentiate with respect to b_1.

We can now proceed to calculate

$$\bar{\mathcal{H}} = \langle \Phi | \tilde{S} \hat{\mathcal{H}} | \Phi \rangle$$
$$= \langle \Phi | \hat{\mathcal{H}}_0 | \Phi \rangle + \frac{\tilde{b}_1}{2} \sum_l \sum_{\rho'} \langle \Phi | s_l^- s_{l+\rho'}^- \hat{\mathcal{H}}_2 | \Phi \rangle$$

The first term is E_g evaluated earlier:

$$\langle \Phi | \hat{\mathcal{H}}_0 | \Phi \rangle = -\frac{Nn}{8}(\Delta + 2b_1)$$

while the term inside the summation in the second term was evaluated in determining b_1 and is given by (using m and ρ instead of l and ρ')

$$\langle \Phi | s_m^- s_{m+\rho}^- \hat{\mathcal{H}}_2 | \Phi \rangle = -\frac{1}{2}[1 - (n+1)b_1^2 - 2(n-1)\Delta b_1].$$

Thus, carrying out the summations,

$$\bar{\mathcal{H}} = -\frac{Nn}{8}(\Delta + 2b_1) - \frac{\tilde{b}_1 Nn}{4}[1 - (n+1)b_1^2 - 2(n-1)\Delta b_1].$$

Differentiating with respect to b_1 and setting this equal to 0 yields Eq. (10.43).

$$-1 + \tilde{b}_1[(n+1)2b_1 + 2(n-1)\Delta] = 0.$$

References

1. Bishop, R.F.: Theor. Chim. Acta **80**, 95 (1991) 109
2. Roger, M., Hetherington, J.H.: Phys. Rev. B **41**, 200 (1990) 110
3. Roger, M., Hetherington, J.H.: Europhys. Lett. **11**, 255 (1990) 110
4. Bishop, R.F., Parkinson, J.B., Xian, Y.: Phys. Rev. B **44**, 9425 (1991) 110
5. Bishop, R.F., Parkinson, J.B., Xian Y.: Phys. Rev. B **46**, 880 (1992) 110, 124, 127, 128
6. Zeng, C., Farnell, D.J.J., Bishop, R.F.: J. Stat. Phys. **90**, 327 (1998) 110
7. Bishop, R.F., Farnell, D.J.J., Krüger, S.E., Parkinson, J.B., Richter, J., Zeng, C.: J. Phys. Condens. Matter **12**, 7601 (2000) 110, 115, 126, 127
8. Farnell, D.J.J., Gernoth, K.A., Bishop, R.F.: J. Stat. Phys. **108**, 401 (2002) 110
9. Farnell, D.J.J., Bishop, R.F.: arxi.org/abs/cond-mat/0311126 (1999) 110
10. Krüger, S.E., Darradi, R., Richter, J., Farnell, D.J.J.: Phys. Rev. B **73**, 094404 (2006) 110, 127
11. Rosenfeld, J., Ligterink, N.E., Bishop, R.F.: Phys. Rev. B **60**, 4030 (1999) 111
12. Barnes, T., Kotchan, D., Swanson, E.S.: Phys. Rev. B **39**, 4357 (1989) 121, 126, 129
13. Sandvik, A.W.: Phys. Rev. B **56**, 11678 (1997) 126
14. Makivic, M.S., Ding, H.Q.: Phys. Rev. B **43**, 3562 (1991) 127
15. Chen, G., Ding, H.-Q., Goddard, W.A.: Phys. Rev. B **46** 2933 (1992) 128
16. Richter, J., Schulenburg, J., Honecker A.: Quantum magnetism in two dimensions: From semi-classical Néel order to magnetic disorder. In: Schollwöck, U., Richter, J., Farnell, D.J.J., Bishop, R.F. (eds.) Quantum Magnetism. Lecture Notes in Physics, vol. 645, pp. 84–153. Springer, Berlin (2004) 130
17. Singh, R.R.P., Gelfand, M.P.: Phys. Rev. B **52**, R15695 (1995) 130